

## TO CIRCULAR MICROCONTACTS DISTRIBUTED OVER ELLIPTICAL CONTOURS

## ON CIRCULAR FLUX TUBES AND HALF SPACES

H. John Saabas \* and M. Michael Yovanovich †

Thermal Engineering Group

Department of Mechanical Engineering

University of Waterloo

Waterloo, Ontario, Canada N2L 3G1

## Abstract

A novel analytic-numerical method is proposed to obtain thermal constriction resistances of multiple regular microcontacts uniformly distributed over macro-elliptical contour regions attached to half spaces or circular flux tubes. The numerical results are in good agreement with a recently published ellipsoidal model. The accuracy of the proposed method is verified by computation of the constriction resistance of a single regular contact on a flux tube, and a single elliptic contact on a half space for which analytical solutions exist. Good agreement is also observed between the numerical results of the method and some electric analog test results for multiple circular contacts on regular contour regions on circular flux tubes.

## Nomenclature

geometric factor between  $i$ th flux annulus and  $j$ th  $z$  depth constants from solving Laplace's equation  
 area of  $j$ th subdivision on simulated flux tube  
 radius of flux tube  
 distance from the center of  $i$ th contact to a point on the flux tube at the  $j$ th  $z$  depth and the  $r$ th azimuth angle  
 distance between the center of  $i$ th contact and the point  $(\rho_m, \phi_m)$  on the plane  $z=mt$   
 complete elliptic integral of 2nd kind  
 complete elliptic integral of first kind  
 thermal conductivity  
 number of azimuth angles used in averaging the PRHF  
 total number of contacts  
 total number of  $z$  divisions used in simulating the flux tube

NPHO

PRHF

 $q_i$  $q_{\rho/i}$  $\bar{q}_i$  $q_{\rho/j}^i$  $q_{\rho/j}$  $q_{\rho/j}^o$  $Q$  $P_{2n}(\cdot)$  $a_i$ 

SEM

 $t$  $\bar{T}_{\text{CONT}}$  $\bar{T}_{\infty}$  $\bar{T}_{\infty}$ 

TCR

 $r$  $R$  $R_{\rho}$  $R_{ho}$  $s$  $v$  $x$ 

## Greek Symbols

 $\alpha_i$  $\beta_i$ number of radial positions used in determining  $\bar{T}_{\infty}$ 

polar radial heat flux

imposed heat flux on  $i$ th annulusheat flux in the  $\rho$  directiondue to  $i$ th flux annulus

average heat flux

acting on the  $i$ th contactheat flux in the  $\rho$  directiondue to the  $i$ th contact in its ownlocal coordinate system at the  $j$ th  $z$ depth and the  $r$ th azimuth anglePRHF due to the  $i$ th contactat the  $j$ th  $z$  depthand the  $r$ th azimuth angleeffective PRHF at the  $j$ th  $z$  depth

total heat flow rate

Legendre polynomial of the

first kind of order  $2n$ 

the polar radial coordinate

of the  $i$ th contact spot

surface element method

dimension used in calculating  $R$ 

average temperature of a set of

contacts

average temperature rise along  $z=mt$ 

due to the imposed annulus

average temperature rise along  $z=mt$ 

due to the contact spots

thermal contact resistance

spherical radial coordinate

thermal constriction resistance

TCR of set of contacts on flux tube

TCR of set of contacts on half space

major axis of elliptic contour region

minor axis of elliptic contour region

independent parameter in

Legendre's equation ( $\cos(\theta)$ )inner radius of  $i$ th imposed flux annulusouter radius of  $i$ th imposed flux

Graduate Research Assistant

Professor, Associate Fellow AIAA

annulus  
 constriction ratio  
 angle from the z-axis in spherical coordinates  
 azimuth angle in spherical coordinates  
 azimuth angle of the *i*th contact spot  
*r*th azimuth angle at which the PRHF is to be calculated  
 polar radial coordinate

### Introduction

Engineering surfaces possess both micro-roughness and macro-out-of-flatness. When two such surfaces are brought into contact under a load, the mechanical interaction is controlled by elastic properties, surface characteristics, geometry and the surface micro-hardness distribution. If both waviness and roughness are present, the result of this interaction is a set of microcontacts distributed over some contour region as depicted in Fig. 1. The solution to this mechanical problem is complex and is not dealt with here.

The presence of the edge of the body is important in the determination of the thermal contact resistance. For this reason the contacts are modelled as being attached to a flux tube. Although the contact geometry described above was the result of a mechanical interaction, this type of modelling is not limited to problems where bodies are brought into contact. Another possible application can be found in microelectronics problems where an array of chips are connected to a circuit board. Each chip can be modelled locally as a discrete heat source.

This thermal problem is a complex 3-D problem which does not lend itself to analytical solution due to the complex nature of the boundary condition, nor to classical numerical techniques such as finite elements due to the vastly different characteristic dimensions of the micro-contacts and the contacting bodies.

Hence, a different approach must be taken to approximate the thermal contact resistance of a set of contacts on an otherwise adiabatic circular flux tube [1]. By using techniques developed for a system of contacts on a half space [2], in conjunction with other half space solutions, a system of contacts on a flux tube can be simulated. The procedure followed was to first place a set of contacts on a half space. The size, distribution, and applied boundary condition (either isoflux or isothermal) of the contacts are assumed to be known. Within the half space, 3 flux annuli were placed external to the desired location of the flux tube (see Fig. 2a). The inner radius of the *i*th annulus is located at  $\alpha_i$ , and the outer radius is at  $\beta_i$ . The uniform heat fluxes acting on these annuli are unknown, but are chosen so as to produce an adiabatic shell at  $\rho = b$  (is a flux tube) in the least squares sense when their temperature distributions are superposed with that due to the set of contacts. By the uniqueness theorem [3], if the superposition solution satisfies Laplace's equation and matches the prescribed boundary conditions, the temperature distribution obtained by superposition will be the same as that of a set of contacts on a flux tube.

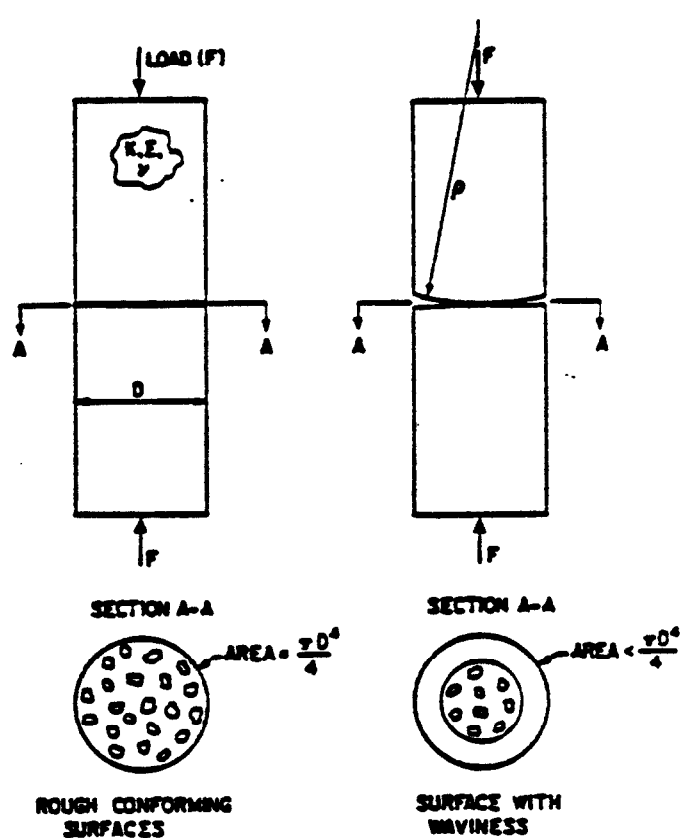


Fig 1 - Contact distribution

Once these heat fluxes are calculated, the temperatures inside the simulated flux tube can be calculated and hence, the thermal contact resistance (TCR) can be computed.

The superposition method was then applied to three test cases:

- (1) One isoflux circular spot concentric on a flux tube
- (2) Electric analog studies of Yip and Venart [8]
- (3) A number of circular isoflux contacts within an elliptical contour

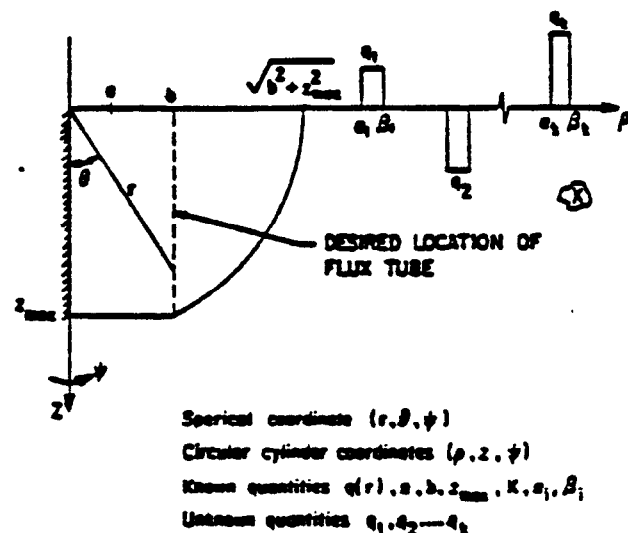


Fig. 2a - Solution space

The solution space used is given in Fig. 2a. The value of  $z_{\max}$  was chosen to be large enough so that there would be no further constriction at that plane or the temperature through the cross section would be uniform. An exact match of the boundary condition of an adiabatic shell at  $\rho = b$  would require a match at an infinite number of points. Hence the boundary condition was approximated by dividing the  $z$  coordinate into  $NN$  equal area subdivisions, striking a radial balance at the mid point of each of these divisions, and then minimizing the sum of the squares of the net heat fluxes (see Fig. 2b). In symbolic form this is given by:

$$f = \sum_{j=1}^{NN} \left\{ q_{\rho j} - q'_{\rho j} \right\}^2 A_j^2 \quad (1)$$

where  $q_{\rho j}$  is the heat flux in the polar radial direction due to the 3 applied flux annuli,  $q'_{\rho j}$  is the effective polar radial heat flux (PRHF) due to the set of contacts and  $A_j$  is the conduction area at the  $j$ th  $z$  depth.  $f$  is the sum of the square of the net heat fluxes.

$q_{\rho j}$  is given by the sum of the polar radial heat fluxes due to the applied annuli, or

$$q_{\rho j} = \sum_{i=1}^3 q_{\rho j i} \quad (2)$$

where  $q_{\rho j i}$  is determined from the temperature solution at a spot on a half space. That is the temperature distribution due to an annulus is given by the temperature distribution due to a flux of  $+q_i$  over a spot of radius  $\beta_i$  and that due to a flux of  $-q_i$  over a spot of radius  $\alpha_i$  (see Fig. 3). The heat flux ( $q_{\rho j i}$ ) is found by using Fourier's Law and is given by [1]

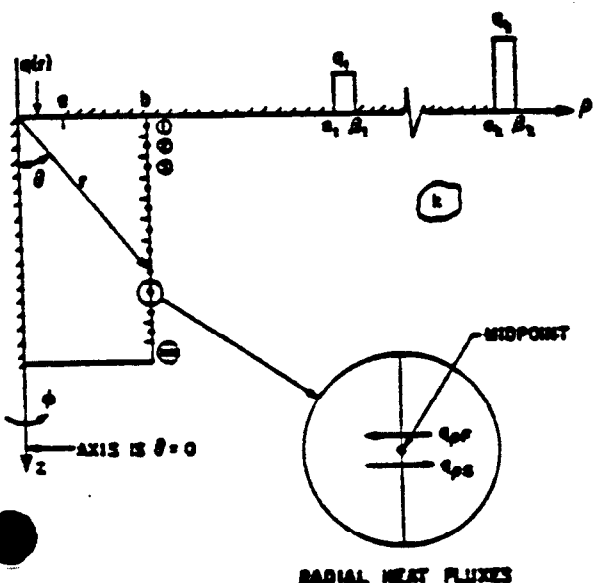


Fig. 2b - Detail of solution space

$$q_{\rho j} = q_i \left\{ \sum_{n=1}^{\infty} A_{2n} 2nr^{2n-1} P_{2n}(z) \left[ \frac{1}{\beta_i^{2n-1}} - \frac{1}{\alpha_i^{2n-1}} \right] \sin(\theta) \right. \\ \left. - \sum_{n=1}^{\infty} A_{2n} r^{2n} \frac{d}{dz} P_{2n}(z) \left[ \frac{1}{\beta_i^{2n-1}} - \frac{1}{\alpha_i^{2n-1}} \right] \frac{z^2 \sin(\theta)}{z} \right\} \quad (3a)$$

where,  $r < \alpha_i$  and  $A_{2n}$  are constants given by equation 3b.

$$A_2 = \frac{1}{2} \\ A_{2n} = \frac{1 \ 1 \ 3 \ (2n-3)}{2 \ 4 \ 6 \ 2n} (-1)^{n+1} \quad (3b)$$

For a given  $r$  and  $\theta$ , or a given  $z$  depth denoted by subscript  $j$ , equation 3a becomes:

$$q_{\rho j} = a_{ij} q_i \quad (4)$$

where  $a_{ij}$  is everything inside the large braces evaluated at the  $j$ th  $z$  depth. Substituting equations 2 and 4 into equation 1, one obtains

$$f = \sum_{j=1}^{NN} \left\{ \sum_{i=1}^3 a_{ij} q_i - q'_{\rho j} \right\}^2 A_j^2 \quad (5)$$

$f$  is then minimized with respect to the  $q_i$ 's as follows

$$\frac{\partial f}{\partial q_i} = 0, \quad i = 1, 2, 3 \quad (6)$$

This results in the following matrix equation:

$$\sum_{j=1}^{NN} a_{ij} \left\{ \sum_{i=1}^3 a_{ij} q_i \right\} = \sum_{j=1}^{NN} a_{ij} q'_{\rho j} \quad i = 1, 2, 3 \quad (7)$$

Again, for a given set of contacts  $q'_{\rho j}$  is known (see Appendix A). Therefore the only unknowns in equation

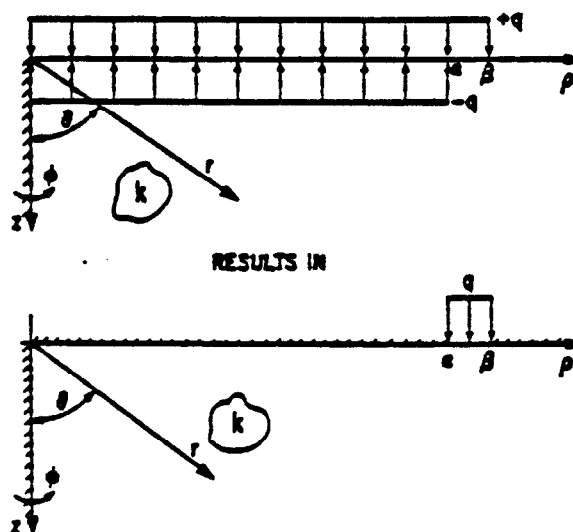


Fig. 3 - Superposition for annular sources

7 are the  $q_i$ 's. These are solved for using Gaussian elimination.

Having determined the fluxes acting on the imposed annuli, temperatures can be calculated and hence, the TCR can be computed. The resistance is defined as:

$$R = \frac{\bar{T}_{CONT} - \bar{T}_{z=1}}{Q} = \frac{t}{k\pi b^2} \quad (8)$$

where  $\bar{T}_{CONT}$  is the average temperature rise of the set of contacts and is given by an area weighted average of the temperature rises of the individual contacts. The temperature rise of each contact is given by the sum of i) its average temperature rise due to its own flux loading, ii) its average temperature rise due to the flux loading on its neighbouring contacts, and iii) the temperature rise due to the imposed annuli. The temperature rise due to its own flux loading and due to the neighbouring contacts' flux loading is determined using the SEM presented in [2]. The temperature rise due to an imposed annulus of flux  $q$  is given by equation 9.

$$T(\rho) = \frac{2}{\pi} \frac{q\beta}{k} E\left(\frac{\rho}{\beta}\right) - \frac{2}{\pi} \frac{q\alpha}{k} E\left(\frac{\rho}{\alpha}\right) \quad (9)$$

The above expression is valid only for values of  $\rho < \alpha$ .  $\rho$  is the polar radial coordinate value of the centroid of the contact in question ( $s_i$ ).

$\bar{T}_{z=1}$  is the average temperature rise at the plane  $z=1$  (see Fig. 2), where it is assumed that the temperature throughout the cross section is uniform. It is given by the superposition of the temperature rises due to the contact spots ( $\bar{T}_{zs}$ ) and that due to the imposed flux annuli ( $\bar{T}_{za}$ ).

$$\bar{T}_{z=1} = \bar{T}_{zs} + \bar{T}_{za} \quad (10)$$

The temperature rise due to one annulus of inner radius  $\alpha$ , and outer radius  $\beta$  is given by equation 11.  $\bar{T}_{zs}$  is given by the sum of the temperature rises due to each annulus.

$$T(r,\theta) = \frac{q\beta}{k} \left\{ 1 - \frac{r}{\beta} P_1(x) + \sum_{n=1}^{\infty} A_{2n} \left(\frac{r}{\beta}\right)^{2n} P_{2n}(x) \right\} - \frac{q\alpha}{k} \left\{ 1 - \frac{r}{\alpha} P_1(x) + \sum_{n=1}^{\infty} A_{2n} \left(\frac{r}{\alpha}\right)^{2n} P_{2n}(x) \right\} \quad r < \alpha \quad (11)$$

The method used to calculate  $\bar{T}_{zs}$  is presented in Appendix B.

$Q$  is the total heat flow rate through the system and is given by the sum of the heat flux acting on each contact multiplied by the contact area.  $\frac{t}{k\pi b^2}$  is the material resistance of a cylinder of length  $t$  and thermal conductivity  $k$ . Finally the resistance is non-dimensionalized with respect to the thermal conductivity and the square root of the contour area.

$$R^* = k\sqrt{A_{contour}}R \quad (12)$$

## Results

The superposition solution discussed above was applied to three test cases.

### Comparison with Exact Solution for One Spot Concentric on a Circular Flux Tube

For the case of one spot on a circular flux tube, the exact solution ( $R_{exact}^*$ ) is determined by solving Laplace's equation in circular cylinder coordinates. The eigenvalue solution is given in [4]. The following table presents TCR results for different constriction ratios ( $\frac{a}{b}$ ) where  $a$  is the radius of the contact spot and  $b$  is the radius of the flux tube. The resistance obtained using the superposition solution is subscripted  $f$ . The agreement between the exact solution and the superposition solution is good.

$\frac{a}{b}$	$R_f^*$	$R_{exact}^*$	% Diff
0.1	0.417	0.416	0.43
0.3	0.295	0.296	-0.19
0.5	0.182	0.181	0.44
0.6	0.131	0.130	0.61
0.7	0.085	0.084	0.59

Table 1 Constriction resistances for one spot on a flux tube

The above table was determined by setting  $b=1, q=1, NN=20, NAZ=1, NPHO=10, NCONT=1, k=1, \alpha_1=3.0, \beta_1 = \alpha_2 = 3.2, \beta_2 = \alpha_3=3.3882, \beta_3=3.5665, z_{max}=2$  and  $t=1$ .  $q_{fj}^*$  was determined using the following 2-D equation:

$$q_{fj}^* = q a \left\{ \sum_{n=1}^{\infty} A_{2n} \frac{a^{2n-1}}{r^{2n}} (2n-1) P_{2n-2}(x) \sin(\theta) + \sum_{n=1}^{\infty} A_{2n} \frac{a^{2n-1}}{r^{2n-1}} \frac{d}{dx} P_{2n-2}(x) \frac{x^2 \sin(\theta)}{z} \right\}$$

This equation is used rather than the expressions given in Appendix A, as the expressions given in Appendix A assume that the spot is at a distance of at least seven spot radii from the flux tube. This assumption is not valid for large values of  $\frac{a}{b}$ . The % Diff in the above table is defined as the flux tube resistance minus the exact resistance all divided by the exact resistance.

comparison with electric analog tests of Yip and Venart [6]

An electric analog study permits the comparison of multicontact problem to a thermal model without having to solve a mechanical problem. The contacts in Yip and Venart's study [6] are isopotential. Comparison of applicable results are given in Table 2. The superposition solution compares favourably to the experimental results.

Test # [6]	$kR$ Expt	$2kR_p$	% Diff
3	0.932	0.923	-0.93
16	0.300	0.293	-2.3
23	0.504	0.514	1.97

Table 2 Comparison with electric analog tests [6]

The test number given corresponds to the test number referenced in [6]. In test #3 nine circular microcontacts of radius 0.059 inches were distributed inside a circular contour region of radius 0.56 inches. One contact was located at the centre of the flux tube with the other eight spaced at one quarter inch intervals along the x and y axes. In test #16 there were nine contacts of radius 0.12 inches, eight of which were equally spaced along the perimeter of a contour region of radius 0.62 inches. The remaining contact was at the centre of the flux tube. Test 16 saw sixteen contacts of radius 0.06 inches equally spaced about the perimeter of a contour region of radius 0.50 inches. In all cases the flux tube radius was 0.99 inches. The superposition solution only considers one half of the total problem. Consequently when comparing to experimental results it must be multiplied by a factor of 2.

#### A Set of Contacts in an Elliptical Contour

The superposition solution was then used to determine the TCR of a set of contacts of radius  $a$ , distributed in an elliptical contour regions and attached to a circular flux tube as depicted in Fig. 4.

The object of this exercise was to put enough contacts inside the elliptical contour region so that the results obtained could be interpreted as the thermal constriction resistance of an isoflux elliptical spot on a circular flux tube. The definition of enough spots was the number of spots required within the elliptical contour region to make it behave like an elliptical spot on a half space. Behaviour is defined as

having equal contact resistances. That is the TCR of the set of contacts is within one percent of the resistance of a continuous elliptical contact, whose constriction resistance is known analytically [3] and is given in equation 13.

$$4k \approx R = \frac{64}{3\pi^3} K \left\{ \left[ 1 - \left( \frac{v}{u} \right)^2 \right]^{\frac{1}{2}} \right\} \quad (13)$$

where  $k$  is the thermal conductivity,  $v$  is the minor axis of the ellipse,  $u$  is the major axis of the ellipse and  $K(\cdot)$  is the complete elliptic integral of the first kind. The SEM developed in [2] can be used to determine the TCR of an arbitrary set of contacts on an otherwise adiabatic half space (subscripted  $h_s$ ). The first step in the analysis is to place a number of circular contacts in an elliptical contour region on an otherwise adiabatic half space so that 10% of the contour region is covered. The theory presented in [2] is then used to predict the TCR. Note, that due to the discrete nature of the contacts, the resistance obtained in this analysis will be greater than the value obtained using equation 13. The number of contacts within the contour region is then increased, and the computations repeated. The resistance obtained using the increased number of contacts is less than the value obtained when only 10% of the contour region was covered. This procedure is repeated until the resistance of the set of contacts is within 1% of the value obtained using equation 13. Equation 13 yields the lower bound on the resistance for a set of contacts within an elliptical region of axes  $u$  and  $v$ .

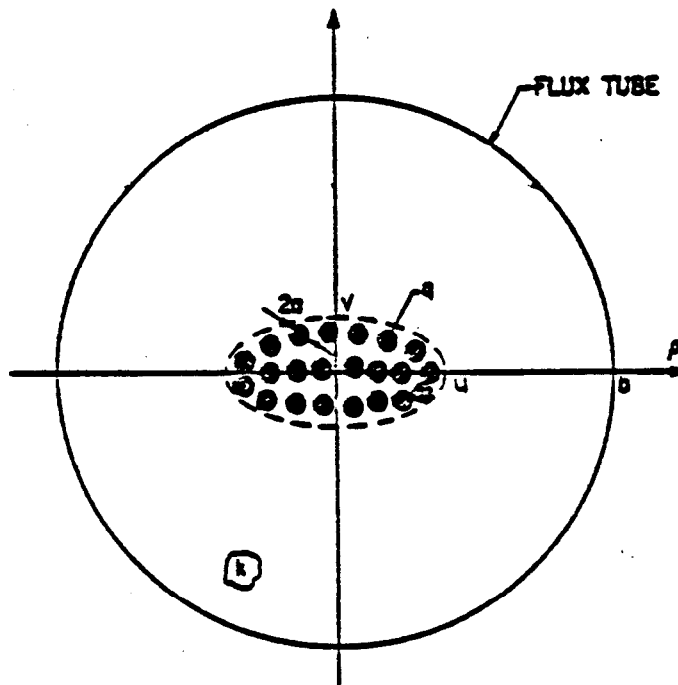


Fig. 4 - Circular microcontacts on elliptical contours on flux tube

The same combinations of contact spots were then used to determine the resistance of a set of contacts in an elliptical contour region on a circular flux tube. These values were obtained using the superposition solution and will now be referred to as the flux tube solution (subscripted  $f$ ). As an exact solution of contact resistance does not exist for the case of a general continuous elliptical spot on a circular flux tube, the only case where a direct comparison to an exact flux tube solution exists is for the special case of a circular contact [4].

A typical set of results of  $R^* = k\sqrt{rv}R$  versus  $N$ , the number of contacts, is given in Tables 3 to 5 for varying elliptical contours. For each elliptical contour the contact distribution was also changed. The radius of the circular contacts ( $a$ ) which are distributed inside the elliptical contour are given at the bottom of the table along with the value of the minor axis of the ellipse ( $v$ ).  $z$  was set to 100. The other parameters were  $b=1000, \alpha_1 = 3000, \beta_1 = \alpha_2 = 3200, \beta_2 = \alpha_3 = 3388, \beta_3 = 3557, NAZ=5, NPHO=6, NN=20$ .

Half Space				Flux Tube		
N	% Area	$R_{hs}^*$	$\frac{R_{hs}^*}{R_f^*}$	N	% Area	$R_f^*$
46	9.2	0.506	1.47	46	9.2	0.580
102	20.4	0.460	1.12	102	20.4	0.433
160	32.0	0.425	1.03	160	32.0	0.397
218	43.6	0.412	1.00	218	43.6	0.384

Table 3 The effect of increasing  $N$  on  $R^*$  for  $v = 20$  and  $a = 2$

The results shown in Tables 3-5 demonstrate that as the number of contacts within a contour region increases (or as more of the contour region is covered with contact spots), the set of contacts starts to behave like a continuous contact. Assuming that if the set of contacts behaves like a continuous contact on a half space they will also behave as such on a flux tube; the flux tube resistance obtained using the largest number of contact spots is a good estimate of the resistance of an elliptical spot on a circular flux tube.

The above procedure of increasing the number of contacts within the elliptical contour until the set of contacts behaved as a continuous contact was repeated for various elliptical contours. The results presented in Table 6 are the resistance values of the contact distributions containing the largest number of contacts used for each elliptical contour.

Half Space				Flux Tube		
N	% Area	$R_{hs}^*$	$\frac{R_{hs}^*}{R_f^*}$	N	% Area	$R_f^*$
62	14.0	0.538	1.18	62	14.0	0.498
106	23.9	0.480	1.06	106	23.9	0.441
150	33.8	0.461	1.01	150	33.8	0.422
180	40.5	0.456	1.00	180	40.5	0.417

Table 4 The effect of increasing  $N$  on  $R^*$  for  $v = 40$  and  $a = 3$

Half Space				Flux Tube		
N	% Area	$R_{hs}^*$	$\frac{R_{hs}^*}{R_f^*}$	N	% Area	$R_f^*$
64	23.0	0.513	1.07	64	23.0	0.452
80	28.8	0.496	1.04	80	28.8	0.434
112	40.3	0.484	1.01	112	40.3	0.422
128	46.1	0.483	1.01	128	46.1	0.421

Table 5 The effect of increasing  $N$  on  $R^*$  for  $v = 100$  and  $a = 6$

The column of Table 6 that presents the ratio of the half space resistance (as determined using the SEM) to the exact resistance (equation 13) demonstrates that a set of contacts can behave as a continuous contact. The entries in the column of  $\frac{R_{hs}^*}{R_f^*}$  for the flux tube results given in Table 6 demonstrate that the assumption of the set of contacts acting as a continuous contact on a flux tube if they act as such on a half space is valid.

As there is no analytical solution for a continuous elliptical contact on a circular flux tube, direct comparison of the results presented in Table 6 to an "exact" expression is not possible. However the ellipsoidal model of Yovanovich et al. [5] predicts the


				Half Space		Flux Tube	
	a	x	v	$R_{\Delta o}^*$	$\frac{R_{\Delta o}^*}{R_v^*}$	$R_{\beta}^*$	$\frac{R_{\beta}^*}{R_v^*}$
218	2	100	20	0.412	1.00	0.384	
180	3	100	40	0.456	1.00	0.417	
136	5	100	80	0.479	1.00	0.424	
128	6	100	100	0.483	1.01	0.421	1.01
144	1.1	20	20	0.484	1.01	0.472	1.01
144	3	200	20	0.357	1.00	0.319	
222	4	300	20	0.330	1.02	0.282	

Table 6 Change in resistance with contour area geometry

constriction resistance of an isothermal ellipse on a square flux tube ( $R_{\Delta o}^*$ ) It can be modified to the isoflux condition and compared against the proposed method.

$$R_{\Delta o}^* = k \sqrt{\pi x v} R_{\Delta o}^T = \frac{1}{4} \frac{\sqrt{\pi v}}{\sqrt{x}} \left\{ \frac{2}{\pi} K(\kappa) - \frac{4}{\pi} \ln \tan \left[ \frac{\pi}{4} + \frac{1}{2} \arcsin \frac{1}{Y} \right] \right\} \quad (14)$$

where,

$$\kappa = \left\{ 1 - \left( \frac{v}{x} \right)^2 \right\}^{\frac{1}{2}} \quad (15)$$

and,

$$Y = \left\{ 1 + \left( \frac{b'}{x} \right)^2 \right\}^{\frac{1}{2}} \quad (16)$$

Since the constriction ratios used are small, a correction of 1.0808 was used to bring the results in line with the isoflux results. Hence,

$$R_{\Delta o}^* \approx 1.0808 R_{\Delta o}^{*T} \quad (17)$$

For small constriction ratios the shape of the flux tube is not important, but rather its area. The results presented in Table 7 are for a square flux tube whose area ( $4b'^2$ ) is set equal to  $\pi b^2$ . Hence  $b'$  is given by:

$$b' = \left( \frac{\pi}{4} \right)^{\frac{1}{2}} b \quad (18)$$

where  $b$  is set to 1000 for computational purposes.

			Eqn 17	Flux Tube	
u	v	$\frac{u}{v}$	$R_{\Delta o}^*$	$R_{\beta}^*$	% Diff
100	20	5	0.381	0.384	0.97
100	40	2.5	0.411	0.417	1.32
100	80	1.25	0.416	0.424	1.95
100	100	1	0.410	0.421	2.5
20	20	1	0.465	0.472	1.51
200	20	10	0.313	0.319	1.72
300	20	15	0.270	0.282	4.4

Table 7 Comparison of superposition method to equation 17

The % Diff is defined as follows:

$$\% \text{ Diff} = \frac{R_{\beta}^* - R_{\Delta o}^*}{R_{\Delta o}^*} \quad (19)$$

The values obtained using equation 17 is consistently less than the value obtained using superposition. This can best be explained by the fact that a square flux tube of area  $\pi b'^2$  is closer to the contact spot than a circular flux tube of the same area.

The superposition technique can be used to determine the TCR of an elliptical spot on a circular flux tube. The solution has been checked against the limiting case of a circle on a circular flux tube, and to the theory of [5] for small constriction ratios. It is believed that the results obtained for the TCR of a set of contacts within an elliptical contour on a circular flux

#### Conclusions

The superposition technique presented in this paper is an approximate technique for determining the TCR of a set of contacts on a flux tube. Comparison of the limiting case of one spot concentric on a circular flux tube was favourable, as was the comparison to some experimental values. Finally the superposition solution was used to determine the TCR of elliptical isoflux spots on circular flux tubes. The agreement was good for the limiting case of circles and matched well with a modified model for an elliptical spot on a square flux tube.

#### Acknowledgements

HJS thanks the Natural Sciences and Engineering Research Council for funding in the form of a Postgraduate Scholarship. MMY thanks the Natural Sciences and Engineering Council for support in the form of an operating grant A7445. HJS would also like to thank Mr. Leonard Kula for his help in the preparation of this document.

## References

- 1) Saabas, H.J., M.A.Sc. Thesis University of Waterloo, 1985
- 2) M.M. Yovanovich, J.C. Thompson and K.J. Negus, "Thermal Resistance of Arbitrarily Shaped Contacts", 3rd Int. Conf. on Numerical Methods in Thermal Problems, Seattle Washington, Aug. 2-5, 1983.
- 3) M.M. Yovanovich, *Advanced Heat Conduction*, Course Notes for ME 651, Dept. of Mech. Eng., Univ. of Waterloo, 1983.
- 4) M.M. Yovanovich, "General Expressions for Circular Constriction Resistances for Arbitrary Flux Distribution", *Radiative Transfer and Thermal Control*, A.M. Smith, Ed., v49 of Progress in Astronautics and Aeronautics, AIAA, New York, 1975 pp 381-396.
- 5) M.M. Yovanovich, G.R. McGee, and M.H. Schankula, "Ellipsoidal Thermal Constriction Model for Crowned Cylinder/Flat Elastic Contact", ASME Paper 84-HT-49, 22nd National Heat Transfer Conf., Niagara Falls NY, Aug. 1984.
- 6) Yip F.C., Venart, J.E.S., "Surface Topography Effects in the Estimation of Thermal and Electrical Contact Resistance", *Proc. Instn Mech Engrs.*, 1967-68, vol 182 pt 3K

## Appendix A - The Calculation of $q'_{pj}$

A multi contact problem is a three dimensional problem. That is the heat flux is dependent on the azimuth angle ( $\phi$ ) as well as  $r$  and  $\theta$  as shown in Fig. 5.

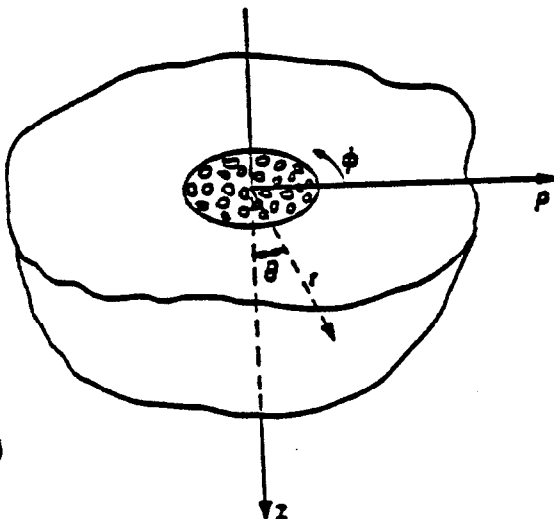


Fig. 5 - Coordinate system

But the technique developed considers the case where

the PRHF is independent of the azimuth angle. Consequently, the PRHF distribution was averaged over the azimuth angle as depicted in Fig. 6.

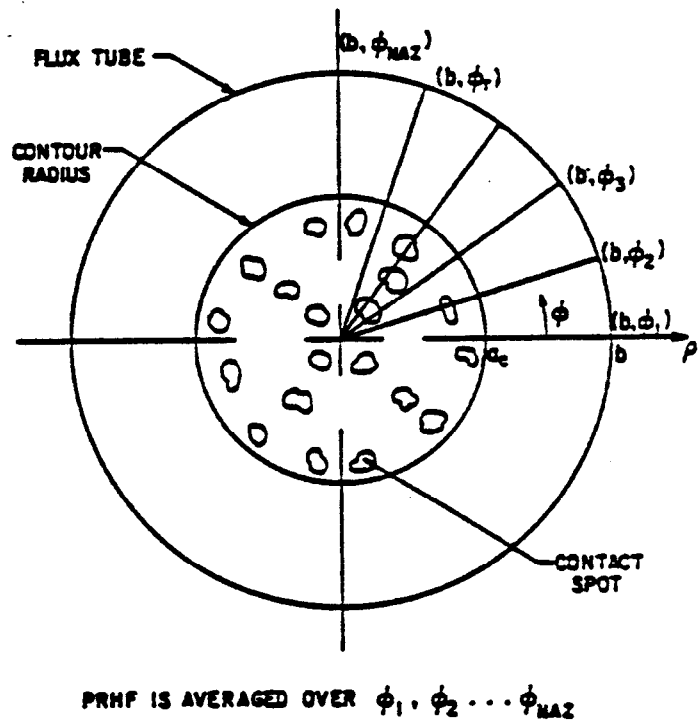


Fig. 6 - Discretization of polar plane

It is believed that this approach is valid if one is trying to determine an integrated parameter such as the TCR, but would introduce error if one was trying to determine a temperature distribution. Although the superposition solution deals with the system of contacts by considering an effective PRHF ( $q'_{pj}$ ), the detail of the contact distribution is considered in the calculation of this number.

In the determination of  $q'_{pj}$ , the solution space is again divided up into  $NN$   $z$  sub divisions but also  $NAZ$  azimuth angles as shown in Fig. 6. The solution procedure is as follows:

- (1) the polar radial heat flux due to the  $i$ th contact is calculated at the  $j$ th  $z$  depth and the  $r$ th azimuth angle in the coordinates local coordinate system as seen in Fig. 7
- (2) as the local polar radial direction is not in the same direction as the flux tube's polar radial coordinate a correction of  $\cos(\lambda_{ir})$  is introduced shown in Fig. 8.
- (3) the PRHF is summed up for all the contacts and all the azimuth angles at each  $z$  depth, and then averaged over the equally spaced azimuth angles. This results in the following expression for  $q'_{pj}$ :

$$q'_{pj} = \frac{1}{NAZ} \sum_{r=1}^{NAZ} \sum_{i=1}^{NCONT} q'_{ri} \cos(\lambda_{ir}) \quad (A.1)$$



where the local Fourier number due to the  $i$ th contact at the  $j$ th  $z$  depth and the  $r$ th azimuth angle ( $q'_{r,j}$ ) is given by:

$$q'_{r,j} = \frac{\bar{q}_i A_i}{2\pi d_{i,j}^2} \sin(\theta_{i,j}) \quad (A.2)$$

where  $\bar{q}_i$  is the average heat flux acting on the  $i$ th contact as determined by a surface element method,  $A_i$  is the area of the  $i$ th contact, and  $d_{i,j}$  and  $\theta_{i,j}$  are defined in the contact's local coordinate system (see Fig. 7). This expression is valid if  $d_{i,j}$  divided by the characteristic dimension of the

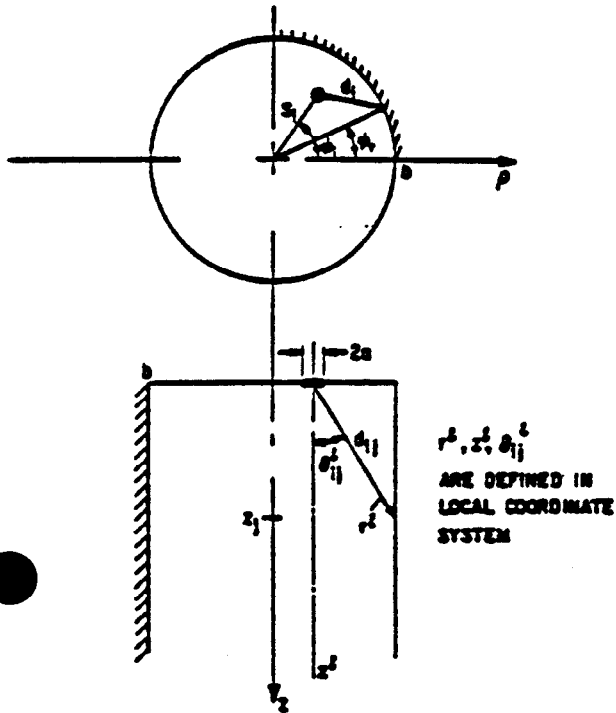


Fig. 7 - Local coordinate system

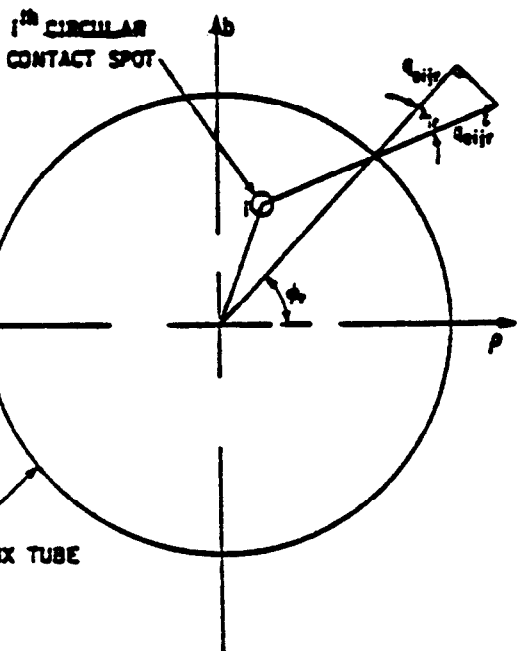


Fig. 8 - The azimuth correction

contact spot is greater than seven. It is at this point that the 1-D solution presented in equation A.2 can replace the complete 2-D solution.

### Appendix B - The determination of $T_{z=t}$

$\bar{T}_{z=t}$  is the average temperature rise on the plane  $z=t$  due to the contact spots. It is found by averaging over the polar radial coordinate and the azimuth angle over the points shown in Fig. 9.

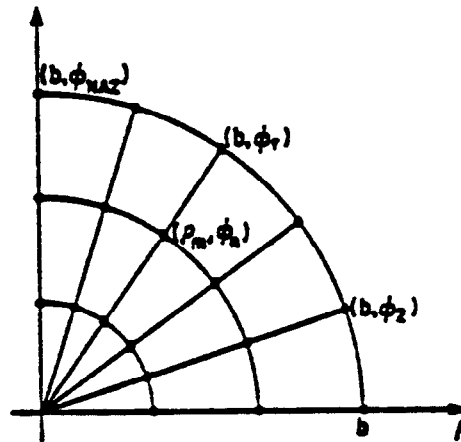


Fig. 9 - The plane  $z=t$

$\bar{T}_{z=t}$  is given by

$$\bar{T}_{z=t} = \frac{1}{NPHO} \frac{1}{NAZ} \sum_{i=1}^{NCONT} \sum_{m=1}^{NPHO} \sum_{n=1}^{NAZ} T_{z=t,ismn} \quad (B.1)$$

where  $NPHO$  is the number of radial positions used in the averaging and  $NAZ$  is the number of azimuth angles used.  $T_{z=t,ismn}$  is the temperature rise at the point  $(\rho_m, \phi_n)$  due to the  $i$ th contact on the plane  $z=t$  and is given by:

$$T_{z=t,ismn} = \frac{\bar{q}_i A_i}{2k\pi d_{ismn}} \quad (B.2)$$

where  $d_{ismn}$  is the distance from the  $i$ th contact to the point  $(\rho_m, \phi_n)$  on the plane  $z=t$ . Again  $A_i$  is the area of the  $i$ th contact. This expression also assumes that  $d_{ismn}$  divided by the characteristic dimension of the contact spot is greater than seven.